Structural and electronic properties of Sc_nO_m ($n = 1 - 3$, $m = 1 - 2n$) clusters: Theoretical study using screened hybrid density functional theory

Yu Yang, Haitao Liu, and Ping Zhang*
LCP, Institute of Applied Physics and Computational Mathematics, P.O. Box 8009, Beijing 100088, People's Republic of China
(Received 12 August 2011; published 16 November 2011)

The structural and electronic properties of small scandium oxide clusters Sc_nO_m ($n = 1 - 3$, $m = 1 - 2n$) are systematically studied within the screened hybrid density functional theory. It is found that the ground states of these scandium oxide clusters can be obtained by the sequential oxidation of small "core" scandium clusters. The fragmentation analysis demonstrates that the ScO, Sc_2O_2, Sc_2O_3, Sc_3O_3, and Sc_3O_4 clusters are especially stable. Strong hybridizations between O-2p and Sc-3d orbitals are found to be the most significant character around the Fermi level. In comparison with standard density functional theory calculations, we find that the screened hybrid density functional theory can correct the wrong symmetries and yield more precise description for the localized 3d electronic states of scandium.

DOI: 10.1103/PhysRevB.84.205430 PACS number(s): 73.22.−f, 36.40.Cg, 36.40.Qv, 71.15.−m

I. INTRODUCTION

Transition-metal oxide clusters have attracted enormous attention because their structural, electronic, and magnetic properties are often quite different from those in their bulk phase.[1–10] For example, small clusters like $(ZnO)_n$, $(V_2O_5)_n$, and $(CrO_3)_n$ form planar structures with very small sizes, and some small clusters present novel magnetic properties.[8,10–12] For scandium (Sc), continuous interest is shown for several reasons. Firstly, Sc is the first transition metal in the periodic table, and thus is always taken as a prototype to study the complex phenomena associated with d-shell electrons.[13] Secondly, Sc oxide nanostructures can be used as catalysts in some reactions like the selective reduction of nitric oxides with methane.[13,14] Thirdly, some Sc oxide clusters have been recognized in the spectra of M-type stars.[13,15] Finally, some Sc oxide clusters can be steadily encapsulated into closed carbon cages of fullerenes to form a novel nanostructure.[16–18]

Small scandium oxide clusters can be prepared by laser ablation of scandium metal in the presence of oxygen-saturated atmosphere.[19–22] With the presence of oxygen or nitrogen oxide gases, scandium oxide clusters ranging from ScO to Sc_3O_6 have already been generated and detected.[22] Many experimental studies have already been applied to study the structural, energetic, vibrational, electronic, and magnetic properties of scandium oxide clusters. For example, the photoionization spectra of Sc_nO were measured and strongly size-dependent ionization potentials were observed.[22,23] For the ScO molecule, the electron-spin resonance and optical spectroscopy in neon and argon matrices revealed that its ground state is a doublet,[22,24] and the molecular bond length and vibrational frequency have been measured to be 1.668 Å and 965 cm^{-1}, respectively.[10,25] Accompanying with these experimental results, lots of theoretical calculations, especially those based on density functional theory (DFT), were also carried out to explore the ground-state electronic structures of scandium oxide clusters. However, most of those studies on Sc oxide clusters were mostly on the standard DFT level, within the local density approximation (LDA) or generalized gradient approximation (GGA). In this paper, we systematically study the atomic and electronic structures of Sc oxide clusters using the screened hybrid density functional theory, which has proven to be able to significantly improve the description of finite, molecular systems, such as atomization energies, bond lengths and vibrational frequencies using standard DFT theories.[26]

II. COMPUTATIONAL METHOD

For extended systems, the ground-state electronic properties can be obtained by solving the Kohn-Sham equation within DFT,[27,28] utilizing the standard approximations for the exchange-correlation (xc) energy functional E_{xc}, i.e., LDA and GGA. One problem of the two most commonly applied functionals is that they rely on the xc energy per particle of the uniform electron gas, and thus are expected to be useful only for systems with slowly varying electron densities (local/semilocal approximation).[29] Although the LDA and GGA functionals have proven to be rather universally applicable in theoretical materials science and achieve fairly good accuracy for ionization energies of atoms, dissociation energies of molecules, and cohesive energies as well as bond lengths and geometries of molecules and solids,[29–32] this unexpectedly good performance for the ground-state properties of many materials is believed to be due to the partial error cancelation in the exchange and correlation energies.[29] In order to improve the performance of DFT on a theoretical basis, one approach is to add a portion of the nonlocal Hartree-Fock (HF) exchange to the local/semilocal approximation for exchange-correlation functional. In computational solid-state physics, a breakthrough was achieved by Heyd, Scuseria, and Ernzerhof, who proposed the HSE03 functional defined by[33–35]

$$E_{\text{xc}}^{\text{HSE03}} = \frac{1}{4}E_x^{\text{HF}}(\text{SR}) + \frac{3}{4}E_x^{\text{PBE}}(\text{SR}) + E_x^{\text{PBE}}(\text{LR}) + E_c^{\text{PBE}}. \quad (1)$$

The HSE03 functional benefits from the range separation of the HF exchange into a short-(SR) and long-range (LR) contribution and replaces the latter by the corresponding DFT exchange part. The HSE03 functional as well as its corrected form, the HSE06 functional,[36] have been extensively applied to calculate ground-state properties of solid and molecular systems as well as adsorption energies for molecules and have proven to be better than the LDA and GGA functionals in describing finite molecular systems.

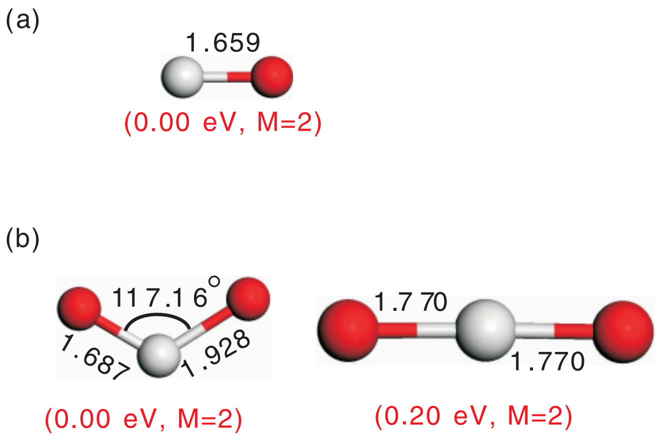

FIG. 1. (Color online) The low-energy structures of (a) ScO and (b) ScO_2 clusters. Grey and red balls represent the scandium and oxygen atoms, respectively. The bond lengths are in units of Å. The number in parenthesis is the relative energy (in eV) with respect to the corresponding ground state. Note that the spin multiplicity is also given in the parenthesis.

The results presented in this work are obtained using the projector augmented wave (PAW) method[37] as implemented in the Vienna *ab initio* simulation package (VASP).[38] For standard DFT calculations, the xc energy is treated within the GGA using the parameterization of Perdew, Burke, and Ernzerhof (PBE)[39,40] to compare with previously published calculations. In the present HSE calculations, the HSE06 hybrid functional[36] is applied, where the range separation parameter is set to 0.2 $Å^{-1}$ for both the semilocal as well as the nonlocal part of the exchange functional. From now on, this particular functional will be referred to as HSE. A plane-wave basis set with a cutoff energy of 400 eV is adopted, and the scandium $3s^2 3p^6 4s^2 3d^1$ and oxygen $2s^2 2p^4$ electrons are treated as fully relaxed valence electrons. A Fermi broadening[41] of 0.05 eV is chosen to smear the occupation of the bands around the Fermi energy (E_f) by a finite-T Fermi function and extrapolating to $T = 0$ K. The supercell containing the scandium oxide clusters is chosen to be without symmetry, and the cell size along each direction is larger than 15 Å. A quasi-Newton algorithm is used to relax the scandium and oxygen ions for all scandium oxide clusters, with the force convergence criteria of 0.01 eV/Åin PBE calculations and 0.03 eV/Åin HSE calculations.

III. RESULTS AND DISCUSSIONS

A. Geometrical structures

Firstly, the ScO and two isomers of ScO_2 are shown in Figs. 1(a) and 1(b), respectively. The optimized bond length of ScO is 1.677 Å in PBE calculation, and 1.659 Å in HSE calculation. The PBE result is in good agreement with former GGA calculations.[10] The HSE06 result is near the ones obtained from the self-consistent field method (SCF)[42] Becke's one-parameter exchange method with Lee-Yang-Parr correlation (B1LYP) calculations.[6,7] Both GGA and HSE06 calculations agree well with the experimental bond length (1.668 Å).[25] Moreover, The vibrational frequency of ScO is 1056 cm^{-1} in HSE calculation, which is near the experimental value of 965 cm^{-1}.

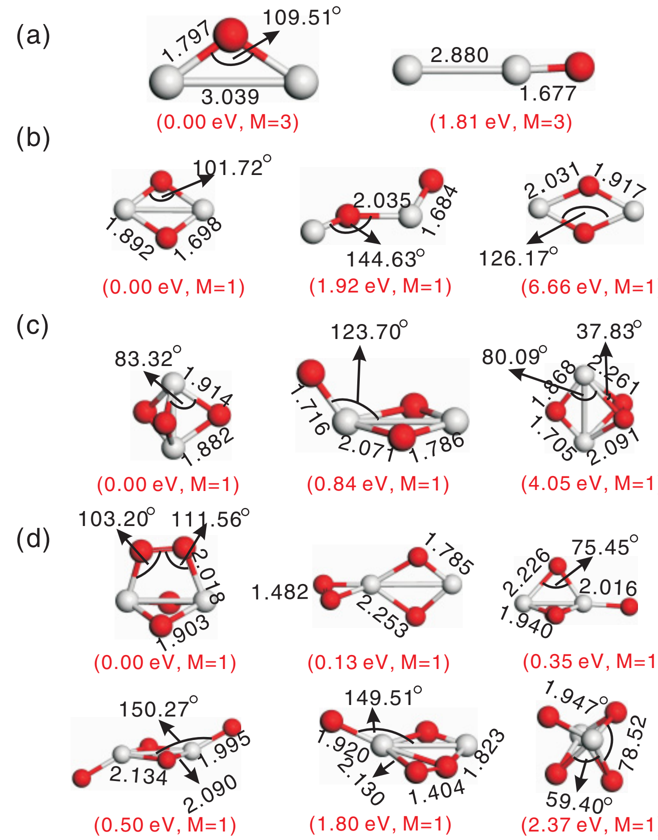

FIG. 2. (Color online) The low-energy structures of (a) Sc_2O, (b) Sc_2O_2, (c) Sc_2O_3, and (d) Sc_2O_4 clusters. Grey and red balls represent the scandium and oxygen atoms, respectively. The bond lengths are in units of Å. The number in parenthesis is the relative energy (in eV) with respect to the corresponding ground state. Note that the spin multiplicity is also given in the parenthesis.

For ScO_2, the obtained ground state is the obtuse triangle structure, with the apex angle of 117.16°. It is interesting to note that these two Sc-O bonds are not equivalent and the bond lengths are 1.687 and 1.928 Å, respectively. In PBE calculations, the triangle is isosceles, with the apex angle of 126.19° and the ScO bond length of 1.781 Å, in agreement with what have been found by using the PBE functional[10] and (Becke's exchange and Perdew-Wangs' correlation) BPW91 functional.[23] It is clear that the HSE06 calculation reduces the symmetry of the ground state. Both GGA and HSE06 demonstrate that the doublet is the most stable electronic state for the ground state of the ScO_2 cluster, in good agreement with the experimental result. The next stable state of ScO_2 is the O-Sc-O linear structure with 0.2 eV higher than the ground state.

The low-lying isomers of Sc_2O_m ($m = 1 - 4$) are presented in Figs. 2(a)–2(d). The ground-state structure of Sc_2O cluster is also an obtuse triangle. The apex angle is 109.51°, and the two Sc-O bonds are both 1.797 Å long, indicating that the cluster has a C_{2v} point symmetry. The ground state of Sc_2O is a triplet, which is in agreement with previous DFT studies.[10] The next stable structure of Sc_2O is linear and has a triplet electronic state. The Sc_2O_2 cluster adopts a distorted square as its ground-state structure. The Sc-O bond lengths are 1.892, 1.698, 1.892, and 1.698 Å, respectively. Since the PBE calculation prefers the rhombus with D_{2h} symmetry, our result is in accordance

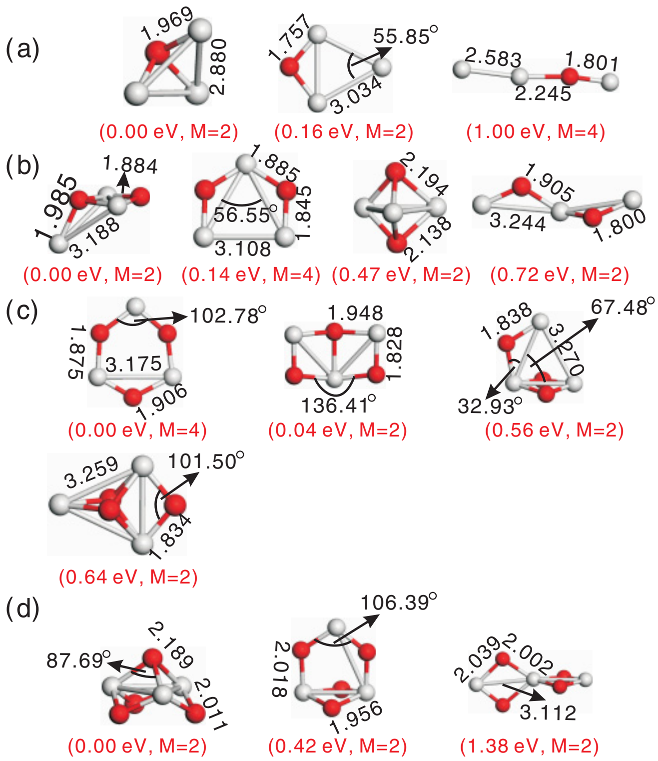

FIG. 3. (Color online) The low-energy structures of (a) Sc_3O, (b) Sc_3O_2, (c) Sc_3O_3, and (d) Sc_3O_4 clusters. Grey and red balls represent the scandium and oxygen atoms, respectively. The bond lengths are in units of Å. The number in parenthesis is the relative energy (in eV) with respect to the corresponding ground state. Note that the spin multiplicity is also given in the parenthesis.

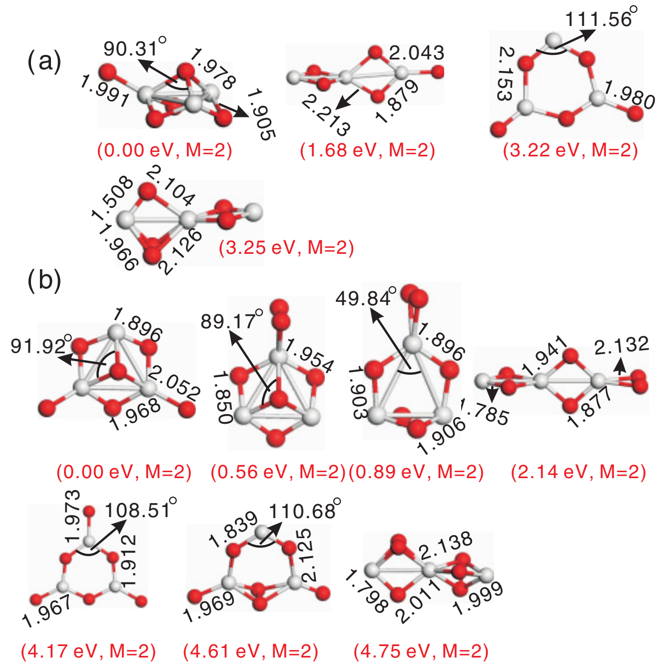

FIG. 4. (Color online) The low-energy structures of (a) Sc_3O_5 and (b) Sc_3O_6 clusters. Grey and red balls represent the scandium and oxygen atoms, respectively. The bond lengths are in units of Å. The number in parenthesis is the relative energy (in eV) with respect to the corresponding ground state. Note that the spin multiplicity is also given in the parenthesis.

with the rule that the HSE06 functional tends to reduce the point group symmetry of some clusters obtained from the PBE calculations. The ground-state of Sc_2O_2 is singlet, and the next stable state is the triplet state of the same structure. The other two structures of Sc_2O_2 in Fig. 2(b) actually have much higher electronic free energies. For Sc_2O_3, the ground-state structure is the singlet trigonal bi-pyramid structure shown in Fig. 2(c). This structure has a D_{3h} symmetry in PBE calculation, which disappears in HSE calculation. Until now, our PBE calculational results are in good agreement with the results reported by Wang *et al.*[10] The main modification of the HSE method, as we can see from the above description, is revealing a lower symmetry for the ground-state structure. In the previous work by Wang *et al.*, the ground-state structure of Sc_2O_4 is the one with a molecular O_2 adsorbing at one corner of the rhombus Sc_2O_2 cluster, which is however, proven to be the next stable structure for Sc_2O_4. The more stable structure we revealed for Sc_2O_4 is the adsorbing structure with an O_2 molecule adsorbing on top of the Sc-Sc bond, as shown in Fig. 2(d). The ground and next stable states of Sc_2O_4 are both singlet.

The Sc_3O cluster has been reported to have a singlet ground state, with the structure of an oxygen atom adsorbing on top of an equilateral scandium triangle.[43] Our result of Sc_3O is the same with previous, in both PBE and HSE calculations. The next stable structure of Sc_3O is the one with an oxygen atom adsorbing at the bottom of an isosceles scandium triangle, having a singlet electronic state and a free electronic energy of 0.16 eV higher than that of the ground-state of Sc_3O. Except for Sc_3O, other Sc_3O_m clusters have seldom been studied before. Only a systematic study on the Sc_3O_6 cluster is reported very recently.[22] The ground-state of Sc_3O_2 is the doublet state of the adsorbing structure of a scandium atom on the Sc_2O_2 cluster. We also notice that there are several structure for the Sc_3O_2 cluster having close free electronic energies, which are thus shown in Fig. 3(b). They are the pentagon, bipyramid, and bitriangle structures, respectively. The Sc_3O_3 cluster adopts a hexagon structure with a fourfold spin multiplicity as its ground state. The smallest O-Sc-O angle is 101.59° in PBE calculation and 102.78° in HSE calculation. We also listed several other structures of Sc_3O_3 in Fig. 3(c), especially the next stable doublet state of the folded rectangular structure, which is only 0.04 eV higher in free electronic energy. For Sc_3O_4, the ground-state structure can be seen as the adsorption of an oxygen atom at the center of the hexagonal Sc_3O_3 cluster or the adsorption of three oxygen atoms at the three bottom sides of the pyramid Sc_3O cluster. The next stable structure of Sc_3O_4, which is 0.42 eV higher in free electronic energy, can be seen as replacing one oxygen atom in the hexagonal Sc_3O_3 cluster with two oxygen atoms.

As shown in Fig. 4(a), the ground-state structure for Sc_3O_5 can be seen as adding an oxygen atom on top of the scandium atom in the ground-state structure of Sc_3O_4. The Sc-O bond lengths become a little smaller than that in Sc_3O_4. The next stable structure of Sc_3O_5 is the adsorption of five oxygen atoms on a Sc_3 linear chain, whose free electronic energy is however, much larger than the ground state. The three lowest-energy structures of Sc_3O_6 are the adsorption structures of 6 oxygen

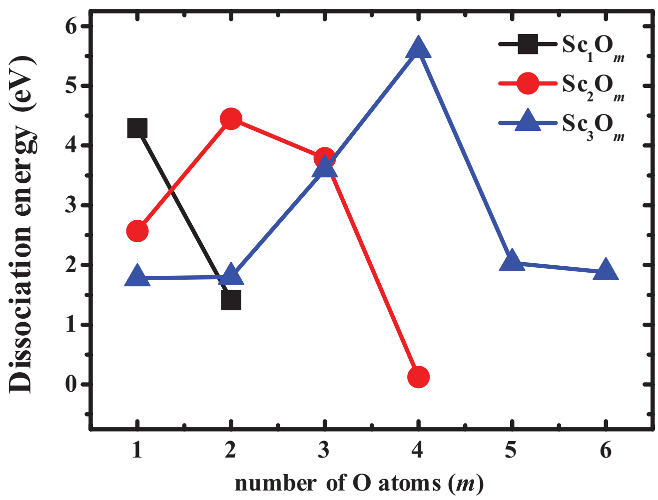

FIG. 5. (Color online) Dissociation energies of the Sc_nO_m clusters as a function of the oxygen atom number m. The corresponding fragmentation channels are listed in Table I.

atoms on the Sc_3 triangle. In the ground state, the oxygen atoms are separated from each other, while in the next and third stable structure, two of the six oxygen atoms bond together. We also find that the structures that contain a Sc_3 chain always have much larger free electronic energies.

B. Important features from the structural studies

Based on the above systematic study of Sc_nO_m clusters, we can see some features for both the oxidation pattern of scandium, and the influences of HSE calculation. For the oxidation of scandium, we conclude two important features. The first one is that the Sc_nO_m cluster can be seen as adding m oxygen atoms to a Sc_n cluster, with the Sc_n cluster to be a scandium dimer for $n = 2$ and a scandium triangle for $n = 3$. The other feature is that the oxygen atoms in the ground states of Sc_nO_m clusters are all bondless with each other, only one O-O bond forms in Sc_2O_4. The fact that oxygen atoms do not bond with each other indicates that scandium oxide clusters are different from lead oxide clusters in which oxygen atoms

TABLE I. The most favorable fragmentation channels and dissociation energies (ΔE, in units of eV) of the Sc_nO_m ($1 \leqslant n \leqslant 3, 1 \leqslant m \leqslant 2n$) clusters. All results are obtained by employing the HSE method.

Cluster	Fragmentation channels	ΔE
ScO	Sc + O	+4.29
ScO_2	ScO + O	+1.41
Sc_2O	Sc + ScO	+2.57
Sc_2O_2	ScO + ScO	+4.45
Sc_2O_3	Sc_2O_2 + O	+3.79
Sc_2O_4	Sc_2O_3 + O	+0.12
Sc_3O	Sc + Sc_2O	+1.78
Sc_3O_2	Sc + Sc_2O_2	+1.80
Sc_3O_3	ScO + Sc_2O_2	+3.60
Sc_3O_4	ScO + Sc_2O_3	+5.60
Sc_3O_5	Sc_3O_4 + O	+2.03
Sc_3O_6	Sc_3O_5 + O	+1.88

can form O_2 or O_3 units.[44] The structural features of Sc_nO_m clusters tell us that they can be built by adding m oxygen atoms separately to a Sc_n cluster.

As for the improvements of the HSE method, the most important one is that the symmetry of the cluster is often lower in the HSE calculation than in the PBE calculation. The lengths of Sc-O bonds always differ from each other in a cluster after geometry optimization using the HSE method. The second feature concluded from the above geometrical studies is that the HSE method does not change the relative stability between different structures. It means that geometry optimization using the PBE-type functional will not yield wrong ground-state structures for scandium oxide clusters. At last, although the electronic structures in PBE and HSE calculations are the same for most Sc_nO_m clusters, we do see differences in the ground-state electronic structures of Sc_3O_2 and Sc_3O_3. In PBE calculations, the magnetic moment is 3 μ_B for Sc_3O_2 and 1 μ_B for Sc_3O_3, and the corresponding magnetic moments obtained from HSE calculations are 1 μ_B for Sc_3O_2 and 3 μ_B for Sc_3O_3.

C. Fragmentation channels and dissociation energies

The stability of scandium oxide clusters with different sizes and stoichiometries is required to illustrate the growth pattern of various nanostructures and to understand even the oxidation behavior of the pristine scandium clusters. On the other hand, the study of the stability is helpful for finding the candidates of the building block of the cluster-assembled materials. Therefore, in the following, we evaluate the fragmentation energy of Sc_nO_m clusters.

When a cluster A is dissociated into B and C fragments (i.e., $A \rightarrow B + C$), the fragmentation energy is defined as $\Delta E = E_B + E_C - E_A$, where the E_B, E_C, and E_A are the free electronic energies of clusters B, C, and A, respectively. In addition, the half of the total energy of an oxygen molecule

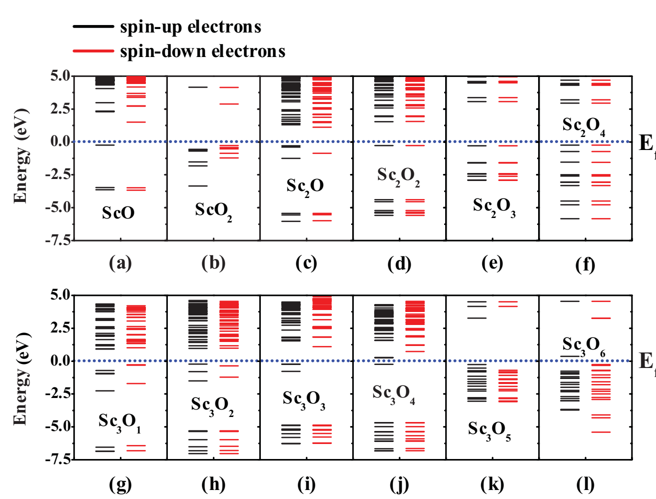

FIG. 6. (Color online) The electronic energy levels for (a) ScO, (b) ScO_2, (c) Sc_2O, (d) Sc_2O_2, (e) Sc_2O_3, (f) Sc_2O_4, (g) Sc_3O, (h) Sc_3O_2, (i) Sc_3O_3, (j) Sc_3O_4, (k) Sc_3O_5, and (l) Sc_3O_6 clusters obtained from HSE calculations. Spin-up and spin-down electronic states are denoted by black and red lines, respectively. The Fermi levels are denoted by the blue dotted lines.

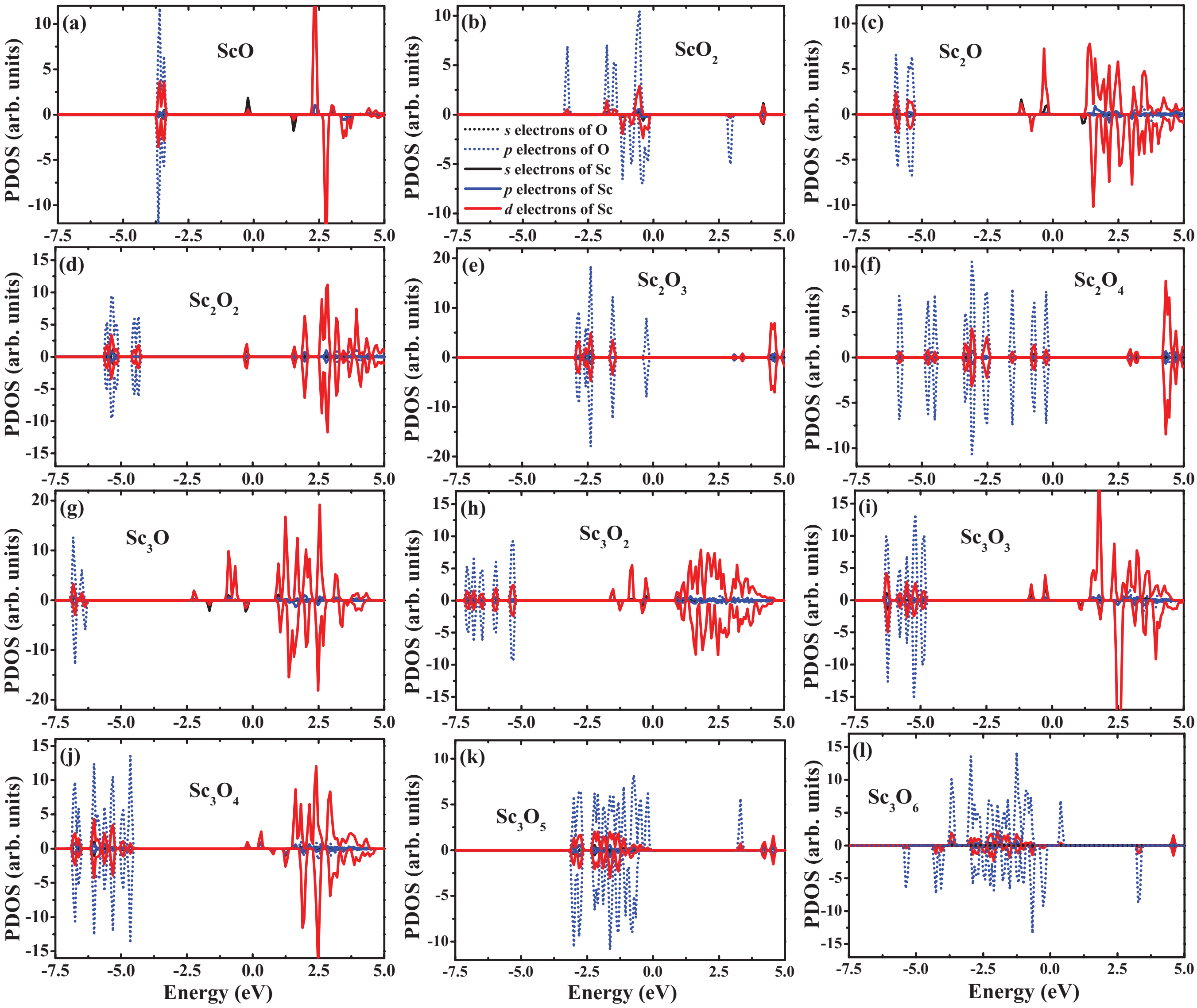

FIG. 7. (Color online) The spin-resolved projected density of states for the (a) ScO, (b) ScO_2, (c) Sc_2O, (d) Sc_2O_2, (e) Sc_2O_3, (f) Sc_2O_4, (g) Sc_3O, (h) Sc_3O_2, (i) Sc_3O_3, (j) Sc_3O_4, (k) Sc_3O_5, and (l) Sc_3O_6 clusters. The Fermi energies are all set to be zero. The electronic states of O and Sc are shown in dotted and solid line, respectively, while *s*, *p*, and *d* electronic states are shown as black, blue, and red lines, respectively.

is adopted as the reference energy for atomic oxygen. Note that a fragmentation process is exothermic (endothermic) if the associated fragmentation energy is negative (positive). The dissociation energy ΔE, defined as the fragmentation energy of the most favorable channel, is calculated and presented in Table I. In general, the cluster with large positive ΔE has great stability, and that with small positive or even negative ΔE is not stable and tends to dissociate. Moreover, the frequently observed fragmentation products are believed to be stable.[44,45] Figure 5 shows the ΔE as a function of the oxygen atom numbers for all clusters, revealing the underlying relationship between stability and stoichiometry of these clusters. The essential features can be discussed as follows.

Firstly, for the dissociation of Sc-rich clusters, the Sc atom is always one of the fragments. To make a further validation, we also study possible fragmentation ways for the Sc_4O cluster, using the HSE calculational method. It is found that the most energetically favored fragmentation channel is $Sc_4O \rightarrow Sc + Sc_3O$, in which a single Sc atom is also a fragment. Secondly, we do not see oxygen molecules in the fragments of Sc_nO_m clusters, the O-rich clusters favor the fragmentation channels that have a single oxygen atom as a product. Lastly, the dissociation energies of ScO, Sc_2O_2, Sc_2O_3, Sc_3O_3, and Sc_3O_4 clusters are larger than 3.60 eV. This indicates that the monoxide-like and sesquioxide-like scandium oxide clusters, and oxide clusters between them are remarkably stable. As a result, these clusters are frequently observed in the fragmentation channels shown in Table I. We also notice that the Sc_3O_4 cluster has an enormous dissociation energy, and is more stable than the monoxide-like Sc_3O_3 cluster. And at another side, the monoxide-like Sc_2O_2 cluster, with a larger dissociation energy, is more stable than the the sesquioxide-like Sc_2O_3 cluster.

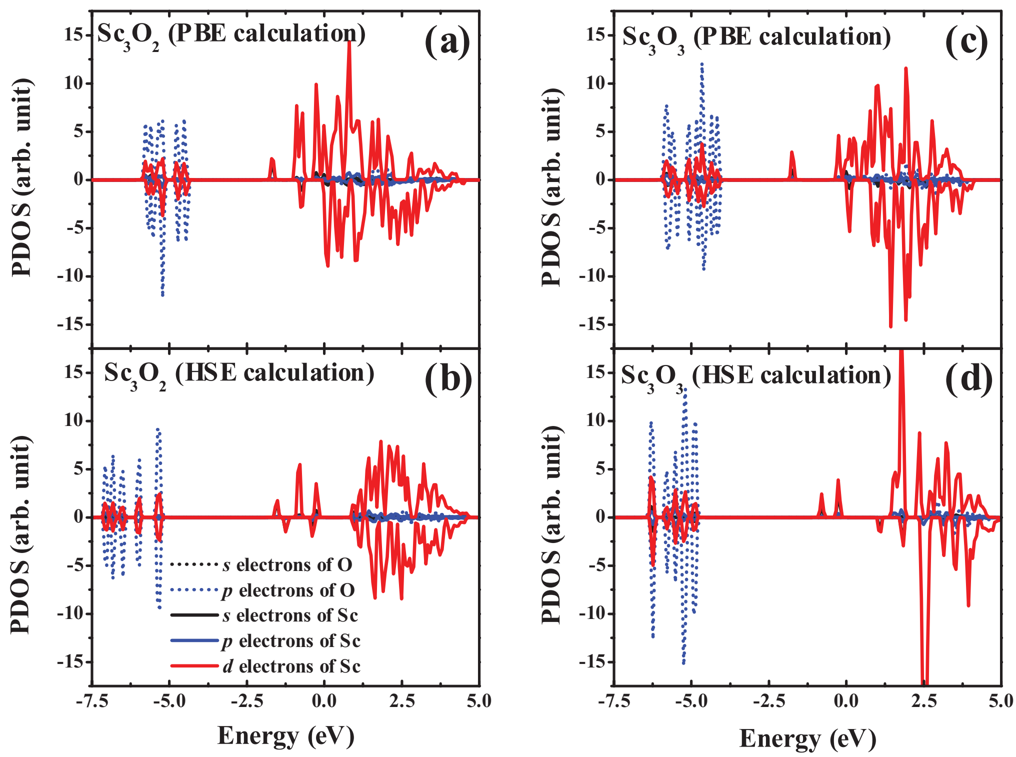

FIG. 8. (Color online) The spin-resolved projected density of states for the Sc_3O_2 cluster in (a) PBE and (b) HSE calculations and the Sc_3O_3 cluster in (c) PBE and (d) HSE calculations. The Fermi energies are all set to be zero. The electronic states of O and Sc are shown in dotted and solid lines, respectively, while s, p, and d electronic states are shown as black, blue, and red lines, respectively.

D. Electronic energy levels

The electronic structures of transition-metal oxide clusters are important characters for their experimental detections and chemical applications. Especially, their magnetic properties are very important to reflect the behavior of the d-shell electrons. We thus calculate the ground-state electronic energy levels of Sc_nO_m clusters using the HSE method. Figure 6 shows the obtained energy levels for different spin-polarized electrons, in which spin-up and spin-down represent the majority and minority spin states, respectively. We find that the Sc_nO_m clusters with odd-number Sc atoms are all magnetic. For the Sc_2O_m clusters, while the Sc_2O is magnetic, the other Sc_2O_2, Sc_2O_3, and Sc_2O_4 clusters are nonmagnetic. The energy gap between the highest occupied molecular orbital (HOMO) and the lowest unoccupied molecular orbital (LUMO) is 1.82, 3.36, and 3.20 eV for the Sc_2O_2, Sc_2O_3, and Sc_2O_4 cluster, respectively. The large band gaps indicate that the Sc_2O_2, Sc_2O_3, and Sc_2O_4 clusters are chemically very stable. In contrast, although the Sc_3O_4 cluster is energetically very stable, its energy gap of spin-up electrons is as small as 0.49 eV, indicating that it is chemically active, and ready to interact with other particles or materials.

To systematically investigate the electronic structures of Sc_nO_m clusters, we then calculate the projected density of states (PDOS) for the Sc_nO_m clusters, which are spin-resolved. Figures 7(a)–7(l) list the obtained s, p, and d PDOS of oxygen and scandium atoms for the Sc_nO_m clusters, respectively. We can clearly see that for all the studied Sc_nO_m clusters, there are strong hybridizations between oxygen-2p and scandium-3d electronic states, and they contribute most of the electronic states around the Fermi energies. For Sc-rich clusters like Sc_2O, Sc_3O, and Sc_3O_2, the HOMO and LUMO are both composed of Sc-3d electrons. For the three nonmagnetic Sc_2O_2, Sc_2O_3, and Sc_2O_4 clusters, the HOMO and LUMO are contributed by O-2p and Sc-3d electrons, respectively, and for O-rich clusters like ScO_2, Sc_3O_5, and Sc_3O_6, the HOMO and LUMO are both 2p electronic states of oxygen. The electronic structure of ScO is, however, different from the other clusters, for its HOMO of spin-up and LUMO of spin-down electrons are contributed by 4s electronic states of scandium.

Since the obtained ground-state spin configurations are different for the Sc_3O_2 and Sc_3O_3 clusters in PBE and HSE calculations, we draw their PDOS together to compare the differences in electronic-state descriptions of PBE and HSE methods, which are shown in Figs. 8(a)–8(d). In the p-d hybridization area from −7.0 to −3.0 eV below the Fermi energies, we can see that the hybridized peaks are more separate in HSE calculations for both the Sc_3O_2 and Sc_3O_3 clusters. The electronic states around the Fermi energy are both Sc-3d states for the two chosen clusters. One can see from Fig. 8 that there are always more localized Sc-3d peaks around the Fermi energy in HSE calculations than in PBE calculations. It means that the HSE method can lead to more localized descriptions for Sc-3d electronic states in Sc_nO_m clusters. Considering that the PBE and other standard GGA methods rely on the xc energy of the uniform electron gas, and thus are expected to be useful only for systems with slowly varying electron densities, we think that the HSE descriptions on the Sc-3d states are more reasonable.

IV. CONCLUSIONS

In this work, first-principles calculations with the HSE method have been performed to study the geometries, stabilities, and electronic structures of small Sc_nO_m clusters ($n = 1 - 3$, $m = 1 - 2n$). Based on an extensive search, it is found that the lowest-energy structures of all these clusters can be obtained by the sequential oxidation of small "core" scandium clusters, with the adsorbing oxygen atoms separating from each other.

The fragmentation analysis reveals that the ScO, Sc_2O_2, Sc_2O_3, Sc_3O_3, and Sc_3O_4 clusters have great stability. This suggests that these clusters might be used as candidates of the building block of cluster-assembled materials. The fragmentation of Sc-rich clusters is found to include a scandium atom as a product, while the fragmentation of O-rich clusters is found to include an oxygen atom as a product. Besides, the above four, extremely stable clusters can also be frequently seen in the fragmentation products of other Sc_nO_m clusters.

Through electronic structure calculations and wave-function analysis, we reveal that most Sc oxide clusters have magnetic ground state except Sc_2O_2, Sc_2O_3, and Sc_2O_4 clusters. The HOMO and LUMO of the three nonmagnetic clusters are composed of O-2p and Sc-3d electronic states, respectively. For the Sc-rich clusters, the HOMO and LUMO are contributed both by Sc-3d electrons, while for O-rich clusters, the HOMO and LUMO are contributed by O-2p electrons.

In comparison with standard PBE calculations, the HSE method is superior because it can correct the wrong symmetries and electronic configurations in PBE results of some clusters.

ACKNOWLEDGMENTS

This work was supported by the NSFC under Grants Nos. 90921003, 10904004, and 11105015.

*zhang_ping@iapcm.ac.cn

[1] S. K. Nayak and P. Jena, Phys. Rev. Lett. **81**, 2970 (1998).
[2] B. V. Reddy and S. N. Khanna, Phys. Rev. Lett. **83**, 3170 (1999).
[3] J. F. Harrwason, Chem. Rev. **100**, 679 (2000).
[4] K. Tono, A. Terasaki, T. Ohta, and T. Kondow, Phys. Rev. Lett. **90**, 133402 (2003).
[5] M. Pykavy and C. van Wüllen, J. Chem. Phys. **120**, 4207 (2004).
[6] Z. W. Qu and G. J. Kroes, J. Phys. Chem. B **110**, 8998 (2006).
[7] E. L. Uzunova, H. Mikosch, and G. S. Nikolov, J. Chem. Phys. **128**, 094307 (2008).
[8] Q. Wang, Q. Sun, and P. Jena, J. Chem. Phys. **129**, 164714 (2008).
[9] D. J. Mowbray, J. I. Martinez, J. M. Garcia Lastra, K. S. Thygesen, and K. W. Jacobsen, J. Phys. Chem. C **113**, 12301 (2009).
[10] Y. B. Wang, X. X. Gong, and J. L. Wang, Phys. Chem. Chem. Phys. **12**, 2471 (2010).
[11] S. F. Vyboishchikov and J. Sauer, J. Phys. Chem. A **105**, 8588 (2001).
[12] S. Li and D. A. Dixon, J. Phys. Chem. A **110**, 6231 (2006).
[13] J. M. Gonzales, R. A. King, and H. F. Schaefer, J. Chem. Phys. **113**, 567 (2000).
[14] M. D. Fokema and J. Y. Ying, Appl. Catal., B **18**, 71 (1998).
[15] P. W. Merrill, A. J. Deutsch, and P. C. Keenan, Astrophys. J. **136**, 21 (1962).
[16] S. Stevenson, M. A. Mackey, M. A. Stuart, J. P. Phillips, M. L. Easterling, C. J. Chancellor, M. M. Olmstead, and A. L. Balch, J. Am. Chem. Soc. **130**, 11844 (2008).
[17] R. Valencia, A. R. Fortea, S. Stevenson, A. L. Balch, and J. M. Poblet, Inorg. Chem. **48**, 5957 (2009).
[18] M. N. Chaur, F. Melin, A. L. Ortiz, and L. Echegoyen, Angew. Chem. Int. Ed. **48**, 7514 (2009).
[19] G. V. Chertihin, L. Andrews, M. Rosi, and C. W. Bauschlicher Jr., J. Phys. Chem. A **101**, 9085 (1997).
[20] H. B. Wu and L. S. Wang, J. Phys. Chem. A **102**, 9129 (1998).
[21] G. P. Kushto, M. Zhou, L. Andrews, and Jr. C. W. Bauchlicher, J. Phys. Chem. A **103**, 1115 (1999).
[22] Y. X. Zhao, J. Y. Yuan, X. L. Ding, S. G. He, and W. J. Zheng, Phys. Chem. Chem. Phys. **13**, 10084 (2011).
[23] G. L. Gutsev, B. K. Rao, and P. Jena, J. Phys. Chem. A **104**, 11961 (2000).
[24] W. J. Weltner, D. J. Mcleod, and P. H. Kasai, J. Chem. Phys. **46**, 3172 (1967).
[25] K. P. Huber and G. Herzberg, *Molecular Spectra and Molecular Structure IV. Constants of Diatomic Molecules* (Van Nostrand, New York, 1979).
[26] R. M. Nieminen, Modell. Simul. Mater. Sci. Eng. **17**, 084001 (2009).
[27] P. Hohenberg and W. Kohn, Phys. Rev. **136**, B864 (1964).
[28] W. Kohn and L. J. Sham, Phys. Rev. **140**, A1133 (1965).
[29] K. Hummer, J. Harl, and G. Kresse, Phys. Rev. B **80**, 115205 (2009).
[30] O. Gunnarsson and B. I. Lundqvist, Phys. Rev. B **13**, 4274 (1976).
[31] R. O. Jones and O. Gunnarsson, Rev. Mod. Phys. **61**, 689 (1989).
[32] W. Kohn, Rev. Mod. Phys. **71**, 1253 (1999).
[33] J. Heyd, G. E. Scuseria, and M. Ernzerhof, J. Chem. Phys. **118**, 8207 (2003).
[34] J. Heyd and G. E. Scuseria, J. Chem. Phys. **121**, 1187 (2004).
[35] J. Heyd, G. E. Scuseria, and M. Ernzerhof, J. Chem. Phys. **124**, 219906 (2006).
[36] A. V. Krukau, O. A. Vydrov, A. F. Izmaylov, and G. E. Scuseria, J. Chem. Phys. **125**, 224106 (2006).
[37] G. Kresse and D. Joubert, Phys. Rev. B **59**, 1758 (1999).
[38] G. Kresse and J. Furthmuller, Phys. Rev. B **54**, 11169 (1996), and references therein.
[39] J. P. Perdew, K. Burke, and M. Ernzerhof, Phys. Rev. Lett. **77**, 3865 (1996).
[40] J. P. Perdew, K. Burke, and M. Ernzerhof, Phys. Rev. Lett. **78**, 1396 (1997).
[41] M. Weinert and J. W. Davenport, Phys. Rev. B **45**, 13709 (1992).
[42] M. Dolg, U. Wedig, H. Stoll, and H. Preuss, J. Chem. Phys. **86**, 2123 (1987).
[43] J. L. Wang, Y. B. Wang, G. F. Wu, X. Y. Zhang, X. J. Zhao, and M. L. Yang, Phys. Chem. Chem. Phys. **11**, 5980 (2009).
[44] H. T. Liu, S. Y. Wang, G. Zhou, J. Wu, and W. H. Duan, J. Chem. Phys. **126**, 134705 (2007).
[45] W. C. Lu, C. Z. Wang, V. Nguyen, M. W. Schmidt, M. S. Gordon, and K. M. Ho, J. Phys. Chem. A **107**, 6936 (2003).